

Ab initio nuclear structure - the large sparse matrix eigenvalue problem

James P. Vary¹, Pieter Maris¹, Esmond Ng², Chao Yang², Masha Sosonkina³

¹Department of Physics, Iowa State University, Ames, IA, 50011 USA

²Computational Research Division, Lawrence Berkeley National Laboratory, Berkeley, CA 94720, USA

³Scalable Computing Laboratory, Ames Laboratory, Iowa State University, Ames, IA, 50011, USA

E-mail: jvary@iastate.edu

Abstract. The structure and reactions of light nuclei represent fundamental and formidable challenges for microscopic theory based on realistic strong interaction potentials. Several *ab initio* methods have now emerged that provide nearly exact solutions for some nuclear properties. The *ab initio* no core shell model (NCSM) and the no core full configuration (NCFC) method, frame this quantum many-particle problem as a large sparse matrix eigenvalue problem where one evaluates the Hamiltonian matrix in a basis space consisting of many-fermion Slater determinants and then solves for a set of the lowest eigenvalues and their associated eigenvectors. The resulting eigenvectors are employed to evaluate a set of experimental quantities to test the underlying potential. For fundamental problems of interest, the matrix dimension often exceeds 10^{10} and the number of nonzero matrix elements may saturate available storage on present-day leadership class facilities. We survey recent results and advances in solving this large sparse matrix eigenvalue problem. We also outline the challenges that lie ahead for achieving further breakthroughs in fundamental nuclear theory using these *ab initio* approaches.

1. Introduction

The structure of the atomic nucleus and its interactions with matter and radiation have long been the foci of intense theoretical research aimed at a quantitative understanding based on the underlying strong inter-nucleon potentials. Once validated, a successful approach promises predictive power for key properties of short-lived nuclei that are present in stellar interiors and in other nuclear astrophysical settings. Moreover, new medical diagnostic and therapeutic applications may emerge as exotic nuclei are predicted and produced in the laboratory. Fine tuning nuclear reactor designs to reduce cost and increase both safety and efficiency are also possible outcomes with a high precision theory.

Solving for nuclear properties with the best available nucleon-nucleon (NN) potentials, supplemented by 3-body (NNN) potentials as needed, using a quantum many-particle framework that respects all the known symmetries of the potentials is referred to as an "*ab initio*" problem and is recognized to be computationally hard. Among the few *ab initio* methods available for light nuclei beyond atomic number $A = 10$, the no core shell model (NCSM) [1] and the no core full configuration (NCFC) [2] methods frame the problem as a large sparse matrix eigenvalue problem one of the foci of the SciDAC-UNEDF program.

2. Nuclear physics goals

Many fundamental properties of nuclei are poorly understood today. By gaining insight into these properties we may better utilize these dense quantum many-body systems to our advantage. A short list of outstanding unsolved problems usually includes the following questions.

- What controls nuclear saturation - the property that the central density is nearly the same for all nuclei?
- How does a successful shell model emerge from the underlying theory, including predictions for shell and sub-shell closures?
- What are the properties of neutron-rich and proton-rich nuclei, which will be explored at the future FRIB (Facility for Rare Isotope Beams)?
- How precise can we predict the properties of nuclei - will it be feasible to use nuclei as laboratories for tests of fundamental symmetries in nature?

The past few years have seen substantial progress but the complete answers are yet to be achieved. We highlight some of the recent physics achievements of the NCSM that encourage us to believe that those major goals may be achievable in the next 10 years. In many cases, we showed the critical role played by 3-body forces and the need for large basis spaces to obtain agreement with experiment.

Since 3-body potentials enlarge the computational requirements by one to two orders of magnitude in both memory and CPU time, we have also worked to demonstrate that similar results may be achieved by suitable adjustments of the undetermined features of the nucleon-nucleon (NN) potential, known as the off-shell properties of the potential. The adjustments were constructed so as to preserve the original high precision description of the NN scattering data. A partial list of the NCSM and NCFC achievements is included below.

- Described the anomaly of the nearly vanishing quadrupole moment of ${}^6\text{Li}$ [3];
- Established need for 3-body potentials to explain, among other properties, neutrino- ${}^{12}\text{C}$ cross sections [4];
- Found quenching of Gamow-Teller (GT) transitions in light nuclei due to effects of 3-body potential [5] (or off-shell modifications of NN potential) plus configuration mixing [6];
- Obtained successful description of $A = 10$ to 13 low-lying spectra with chiral NN + NNN interactions [7];
- Explained ground state spin of ${}^{10}\text{B}$ by including chiral NNN interaction [7].

We have identified several major near-term physics goals on the path to the larger goals listed above. These include:

- Evaluate the properties of the Hoyle state in ${}^{12}\text{C}$ and the isoscalar quadrupole strength function in ${}^{12}\text{C}$ to compare with inelastic α scattering data;
- Explain the lifetime of ${}^{14}\text{C}$ (5730 years) which depends sensitively on the nuclear wavefunction;
- Calculate the properties of the Oxygen isotopes out to the neutron drip line;
- Solve for nuclei surrounding shell closure in order to understand the origins shell closures.

Preliminary results for these goals are encouraging and will be reported when we obtain additional results closer to convergence.

3. Recent NCFC results

Within the NCFC method, we adopt the harmonic oscillator (HO) single particle basis which involves two parameters and we seek results independent of those parameters either directly in a sufficiently large basis or via extrapolation to the infinite basis limit. The first parameter $\hbar\Omega$ specifies the HO energy, the spacing between major shells. Each shell is labeled uniquely by the quanta of its orbits $N = 2n + l$ (orbits are specified by quantum numbers n, l, j, m_j) which begins with 0 for the lowest shell and increments in steps of unity. Each unique arrangement of fermions (neutrons and protons) within the HO orbits that is consistent with the Pauli principle, constitutes a many-body basis state. Many-body basis states satisfying chosen symmetries are employed in evaluating the Hamiltonian H in that basis. The second parameter is N_{\max} which limits the total number of oscillator quanta allowed in the many-body basis states and thus limits the dimension D of the Hamiltonian matrix. N_{\max} is defined to count the total quanta above the minimum for the specific nucleus needed to satisfy the Pauli principle.

3.1. Quadrupole moment of ${}^6\text{Li}$

Experimentally, ${}^6\text{Li}$ has a surprisingly small quadrupole moment, $Q = -0.083 e \text{ fm}^2$. This means that there are significant cancellations between contributions to the quadrupole moment from different parts of the wave function. In Ref. [3] the NCSM was shown to agree reasonably well with the data using a nonlocal NN interaction. Here we employ the realistic JISP16 NN potential from inverse scattering that provides a high-quality description of the NN data [8]. This NN potential is sufficiently well-behaved that we may obtain NCFC results for light nuclei [2]. Indeed, the left panel of Fig. 1 shows smooth uniform convergence of the ground state energy of ${}^6\text{Li}$. The quadrupole moment does not exhibit the same smooth and uniform convergence. Nevertheless, the results for $15 \text{ MeV} < \hbar\Omega < 25 \text{ MeV}$ where the ground state energy is closest to convergence, strongly suggest a quadrupole moment in agreement with experiment.

3.2. Beryllium isotopes

Next, we use the Be isotopes to portray features of the physics results and illustrate some of the computational challenges, again with the JISP16 nonlocal NN potential [8]. Fig. 2 displays the NCFC results for the lowest states of natural and unnatural parity respectively in a range of Be isotopes along with the experimental ground state energy. Since our approach is guaranteed to provide an upper bound to the exact ground state energy for the chosen Hamiltonian, each point displayed for a particular value of N_{\max} represents the minimum value as a function of $\hbar\Omega$

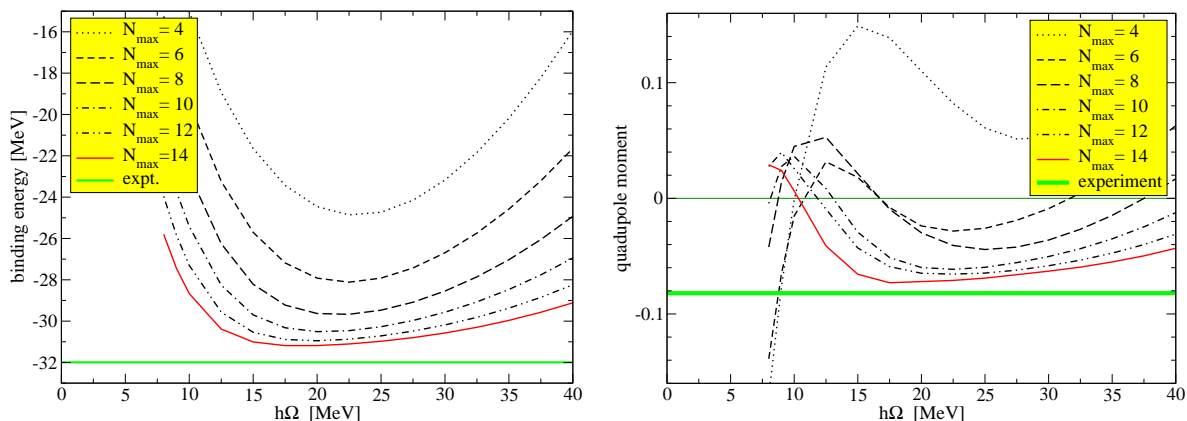


Figure 1. Ground state energy of ${}^6\text{Li}$ (left) and quadrupole moment (right) obtained with the JISP16 NN potential as function of $\hbar\Omega$ for several values of N_{\max} .

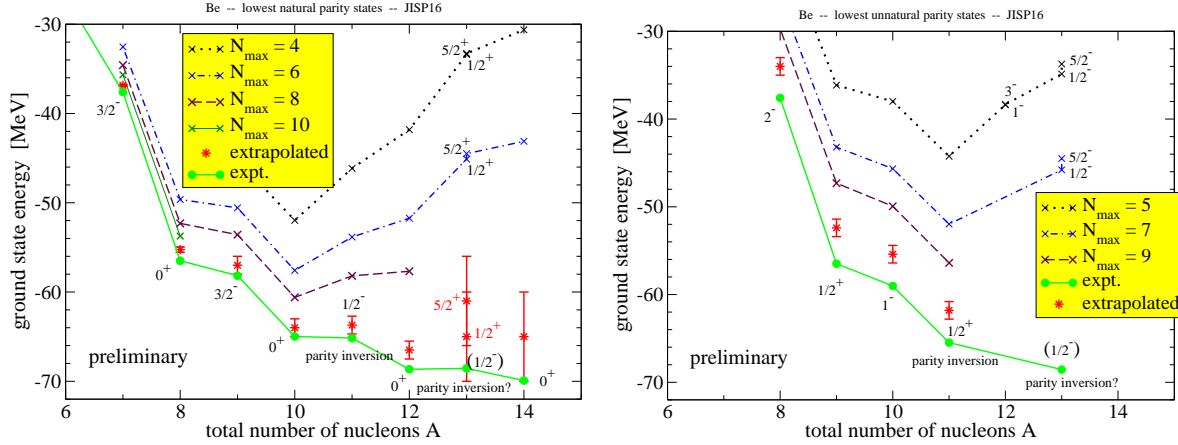


Figure 2. Lowest natural (left) and unnatural (right) states of Be isotopes obtained with the JISP16 NN potential. Extrapolated results and their assessed uncertainties are presented as red points with error bars.

obtained in that basis space.

In small model spaces, $N_{\max} = 4$ and 5 , the calculations suggest a "U-shaped" curve for the binding energy as function of A , the number of nucleons, whereas experimentally, the ground state energy keeps decreasing with A , at least over the range in A shown in Fig. 2. However, as one increases N_{\max} , the calculated results get closer to the experimental values. In order to obtain the binding energies in the full configuration space (NCFC), we can use an exponential fit to a set of results at 3 or 4 subsequent N_{\max} values [2]. After performing such an extrapolation to infinite model space, our calculated results follow the data very closely as function of A .

In both panels of Fig. 2, the dimensions increase dramatically as one increases N_{\max} or increases atomic number A . Detailed trends will be presented in the next section. The consequence is that results terminate at lower A as one increases N_{\max} . Additional calculations are in process in order to reduce the uncertainties in the extrapolations.

We note that the ground state spins are predicted correctly in all cases except $A = 11$ (and possibly at $A = 13$, where the spin-parity of the ground state is not well known experimentally) where there is a reputed "parity inversion". In this case a state of "unnatural parity", one involving at least one particle moving up one HO shell from its lowest location, unexpectedly becomes the ground state. While Fig. 2 indicates we do not reproduce this parity inversion, we do notice, however, that the lowest states of natural and unnatural parity lie very close together. This indicates that small corrections arising from neglected effects, such as three-body (NNN) potentials and/or additional contributions from larger basis spaces could play a role here. We are continuing to investigate these improvements.

4. Computer Science and Applied Math challenges

We outline the main factors underlying the need for improved approaches to solving the nuclear quantum many-body problem as a large sparse matrix eigenvalue problem. Our goals require results as close to convergence as possible in order to minimize our extrapolation uncertainties. According to current experience, this requires the evaluation of the Hamiltonian in as large a basis as possible, preferably with $N_{\max} \geq 10$, in order to converge the ground state wavefunction.

The dimensions of the Hamiltonian matrix grow combinatorially with increasing N_{\max} and with increasing atomic number A . To gain a feeling for that explosive growth, we plot in Fig. 3 the matrix dimension (D) for a wide range of Oxygen isotopes. In each case, we select the "natural parity" basis space, the parity that coincides with the lowest HO configuration for that

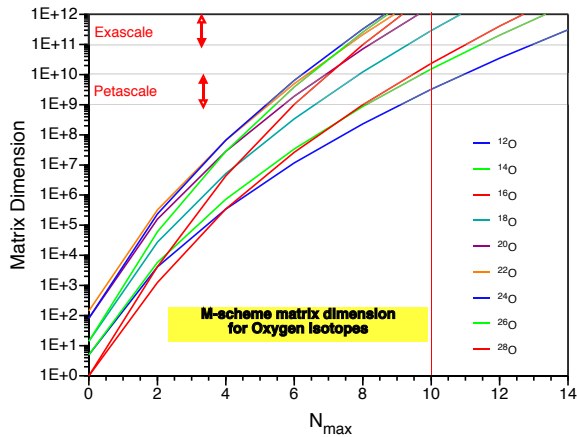


Figure 3. Matrix dimension versus N_{\max} for stable and unstable Oxygen isotopes. The vertical red line signals the boundary where reasonable convergence emerges on the right of it.

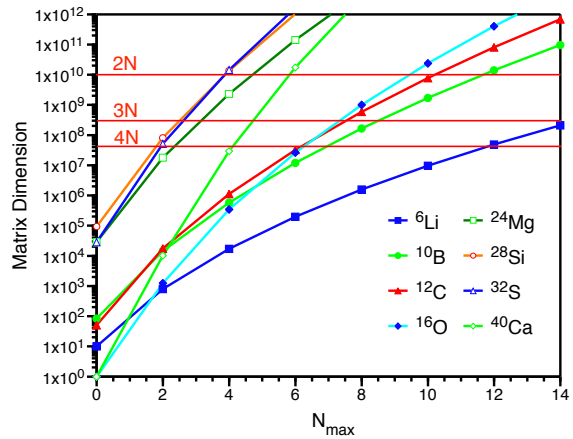


Figure 4. Matrix dimension versus N_{\max} for a sample set of stable $N=Z$ nuclei up to $A = 40$. Horizontal lines show expected limits of Petascale machines for specific ranks of the potentials (“ $2N$ ”= NN , “ $3N$ ”= NNN , etc).

nucleus. The heavier of these nuclei have been the subject of intense experimental investigation and it is now believed that ^{28}O is not a particle-stable nucleus even though it is expected to have a doubly-closed shell structure according to the phenomenological shell model. It would be very valuable to have converged *ab initio* NCFC results for ^{28}O to probe whether realistic potentials are capable of predicting its particle-unstable character.

We also include in Fig. 3 the estimated range that computer facilities of a given scale can produce results with our current algorithms. As a result of these curves, we anticipate well converged NCFC results for the first three isotopes of Oxygen will be achieved with Petascale facilities since their curves fall near or below the upper limit of Petascale at $N_{\max} = 10$.

Dimensions of the natural parity basis spaces for another set of nuclei ranging up to $A = 40$ are shown in Fig. 4. In addition, we include estimates of the upper limits reachable with Petascale facilities depending on the rank of the potential. It is important to note that theoretically derived $4N$ interactions are expected to be available in the near future. Though relatively less important than $2N$ and $3N$ potentials, their contributions are expected to grow dramatically with increasing A .

A significant measure of the computational burden is presented in Figs. 5 and 6 where we display the number of non-zero many-body matrix elements as a function of the matrix dimension (D). These results are for representative cases and show a useful scaling property. For Hamiltonians with NN potentials, we find a useful fit $F(D)$ for the non-zero matrix elements with the function

$$F(D) = D + D^{1 + \frac{12}{14 + \ln D}}. \quad (1)$$

The heavier systems displayed tend to be slightly below the fit while the lighter systems are slightly above the fit. The horizontal red line indicates the expected limit of the Jaguar facility (150,000 cores) running one of these applications assuming all matrix elements and indices are stored in core. By way of contrast, we portray the more memory-intensive situation with NNN potentials in Fig. 6, where we retain the fitted curve of Fig. 5 for reference. The horizontal red line indicates the same limit shown in Fig. 5.

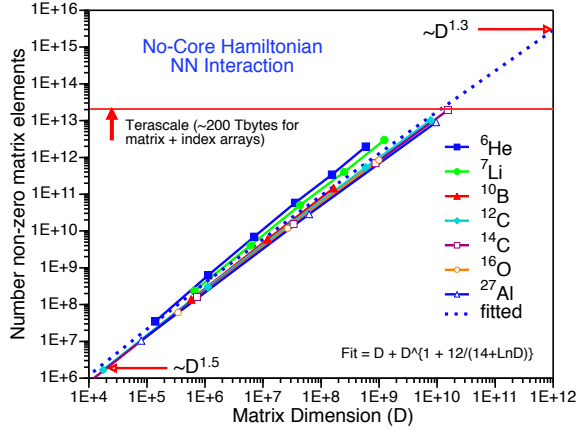


Figure 5. Number of nonzero matrix elements versus matrix dimension (D) for an NN potential and for a selection of light nuclei. The dotted line depicts a function describing the calculated points.

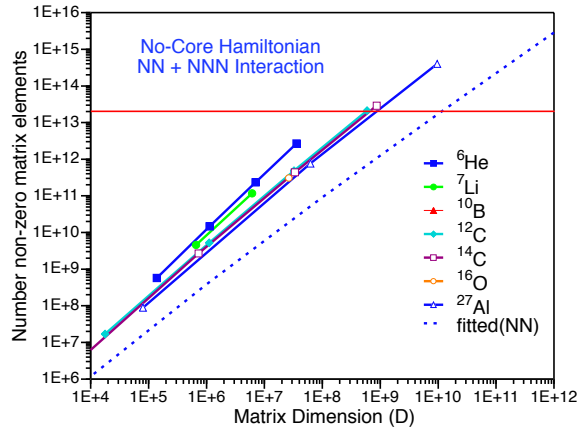


Figure 6. Same as Fig. 5 but for an NNN potential. The NN dotted line of Fig. 5 is repeated as a reference. The NNN slope and magnitude are larger than the NN case. The NNN case is larger by a factor of 10-100.

nucleus	N_{\max}	dimension	2-body	3-body	4-body
${}^6\text{Li}$	12	$4.9 \cdot 10^6$	0.6 GB	33 TB	590 TB
${}^{12}\text{C}$	8	$6.0 \cdot 10^8$	4 TB	180 TB	4 PB
${}^{12}\text{C}$	10	$7.8 \cdot 10^9$	80 TB	5 PB	140 PB
${}^{16}\text{O}$	8	$9.9 \cdot 10^8$	5 TB	300 TB	5 PB
${}^{16}\text{O}$	10	$2.4 \cdot 10^{10}$	230 TB	12 PB	350 PB
${}^8\text{He}$	12	$4.3 \cdot 10^8$	7 TB	300 TB	7 PB
${}^{11}\text{Li}$	10	$9.3 \cdot 10^8$	11 TB	390 TB	10 PB
${}^{14}\text{Be}$	8	$2.8 \cdot 10^9$	32 TB	1100 TB	28 PB
${}^{20}\text{C}$	8	$2 \cdot 10^{11}$	2 PB	150 PB	6 EB
${}^{28}\text{O}$	8	$1 \cdot 10^{11}$	1 PB	56 PB	2 EB

Table 1. Table of storage requirements of current version of MFDn for a range of applications. Roughly speaking, entries up to 400TB imply Petascale while entries above 1PB imply Exascale facilities will likely be required.

Looking forward to the advent of exascale facilities and the development of 4N potentials, we present in Table 1 the matrix dimensions and storage requirements for a set of light nuclei for potentials ranging from 2N through 4N.

5. Algorithms of MFDn

Our present approach embodied in the code Many Fermion Dynamics - nuclear (MFDn) [9, 10, 11] involves several key steps:

- (i) enumerate the single-particle basis states for the neutrons and the protons separately with good total angular momentum projection m_j ,
- (ii) enumerate and store the many-body basis states subject to user-defined constraints and symmetries such as N_{\max} , parity and total angular momentum projection M ,

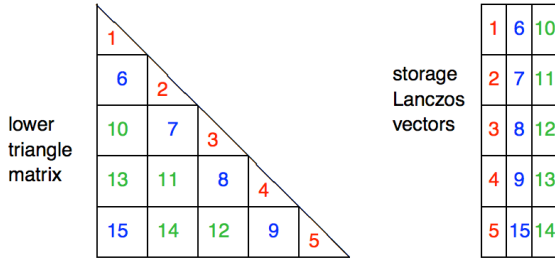


Figure 7. MFDn scheme for distributing the symmetric Hamiltonian matrix over $n(n+1)/2$ PE's and partitioning the Lanczos vectors. We use $n = 5$ "diagonal" PE's in this illustration.

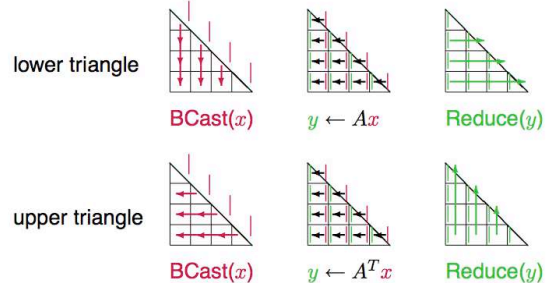


Figure 8. MFDn scheme for performing the Lanczos iterations based on the Hamiltonian matrix stored in $n(n+1)/2$ PE's. We use $n = 4$ "diagonal" PE's in this illustration.

- (iii) evaluate and store the many-nucleon Hamiltonian matrix in this many-body basis using input files for the NN (and NNN interaction if elected),
- (iv) obtain the lowest converged eigenvalues and eigenvectors using the Lanczos algorithm with a distributed re-orthonormalization scheme,
- (v) transform the converged eigenvectors from the Lanczos vector space to the original basis and store them in a file,
- (vi) evaluate a suite of experimental observables using the stored eigenvectors.

All these steps, except the first, which does not require any significant amount of CPU time, are parallelized using MPI. Fig. 7 presents the allocation of processors for computing and storing the many-body Hamiltonian on $n(n+1)/2$ processors. (We illustrate the allocation with 15 processors so the pattern is clear for an arbitrary value of n .) We assume a symmetric Hamiltonian matrix and compute/store only the lower triangle.

In step two, the many-body basis states are round-robin distributed over the n diagonal processors. Each vector is also distributed over n processors, so we can (in principle) deal with arbitrary large vectors. Because of the round-robin distribution of the basis states, we obtain excellent load-balancing; however, the price we pay is that any structure in the sparsity pattern of the matrix is lost. We have implemented multi-level blocking procedures to enable an efficient determination of the non-zero matrix elements to be evaluated. These procedures have been presented recently in Ref. [11].

After the determination and evaluation of the non-zero matrix elements, we solve for the lowest eigenvalues and eigenvectors using an iterative Lanczos algorithm, step four. The matvec operation, and its communication patterns, for each Lanczos iteration is shown in Fig. 8 where two sets of operations account for the storage of only the lower triangle of the matrix.

MFDn also employs a distributed re-orthonormalization technique developed specifically for the parallel distribution shown in Fig. 7. After the completion of the matvec, the new elements of the tridiagonal Lanczos matrix are calculated on the diagonals. The (distributed) normalized Lanczos vector is then broadcast to all processors for further processing. Each previously computed Lanczos vector is stored on one of $(n+1)/2$ groups of n processors. Each group

receives the new Lanczos vector, computes the overlaps with all previously stored vectors within that group, and constructs a subtraction vector, that is, the vector that needs to be subtracted from the Lanczos vector in order to orthogonalize it with respect to the Lanczos vectors stored in that group. These subtraction vectors are accumulated on the n diagonal processors, where they are subtracted from the current Lanczos vector. Finally, the orthogonalized Lanczos vector is re-normalized and broadcast to all processors for initiating the next matvec. One group is designated to also store that Lanczos vector for future re-orthonormalization operations.

The results so far with this distributed re-orthonormalization appear stable with respect to the number of processors over which the Lanczos vectors are stored. We can keep a considerable number of Lanczos vectors in core, since all processors are involved in the storage, and each part of a Lanczos vector is stored on one and only one processor. For example, we have run 5600 Lanczos iterations on a matrix with dimension 595 million and performed the distributed re-orthonormalization using 80 groups of stored Lanczos vectors. We converged about 450 eigenvalues and eigenvectors. Tests of the converged states, such as measuring a set of their symmetries, showed they were reliable. No converged duplicate eigenstates were generated. Test cases with dimensions of ten to forty million have been run on various numbers of processors to verify the strategy produces stable results independent of the number of processors. A key element for the stability of this procedure is that the overlaps and normalization are calculated in double precision, even though the vectors (and the matrix) are stored in single precision. Furthermore, there is of course a dependence on the choice of initial pivot vector; we favor a random initial pivot vector.

6. Accelerating convergence

We are constantly seeking new ideas for accelerating convergence as well as saving memory and CPU time. The situation is complicated by the wide variety of strong interaction Hamiltonians that we employ and we must simultaneously investigate theoretical and numerical methods for "renormalizing" (softening) the potentials. Softening an interaction reduces the magnitude of many-body matrix elements between very different basis states such as those with very different total numbers of HO quanta. However, all methods to date soften the interactions at the price of increasing their complexity. For example, starting with a strong NN interaction, one renormalizes it to improve the convergence of the many-body problem with the softened NN potential [12] but, in the process, one induces a new NNN potential that is required to keep the final many-body results invariant under renormalization. In fact, $4N$ potentials and higher are also induced[7]. Given the computational cost of these higher-body potentials in the many-body problem as described above, it is not clear how much one gains from renormalization - for some NN interactions it may be more efficient to attempt larger basis spaces and avoid the renormalization step. This is a current area of intense theoretical research.

In light of these features of strongly interacting nucleons and the goal to proceed to heavier nuclei, it is important to investigate methods for improving convergence. A number of promising methods have been proposed and each merits a significant research effort to assess their value over a range of nuclear applications. A sample list includes:

- Symplectic no core shell model (SpNCSM) - extend basis spaces beyond their current N_{\max} limits by adding relatively few physically-motivated basis states of symplectic symmetry which is a favored symmetry in light nuclei [13]
- Realistic single-particle basis spaces [14]
- Importance truncated basis spaces [15]
- Monte Carlo sampling of basis spaces [16, 17]
- Coupled total angular momentum J basis space

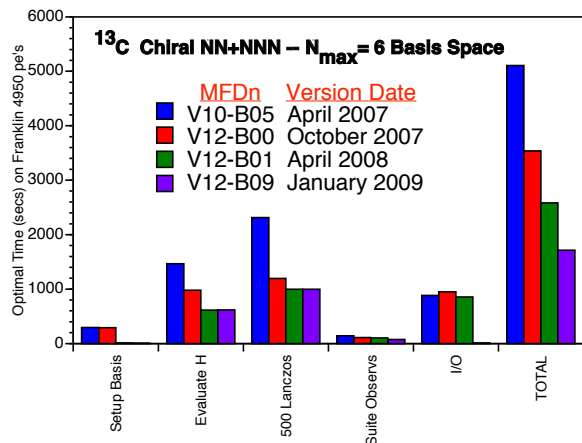


Figure 9. Performance improvement of MFDn over a 2 year span displayed for major sections of the code.

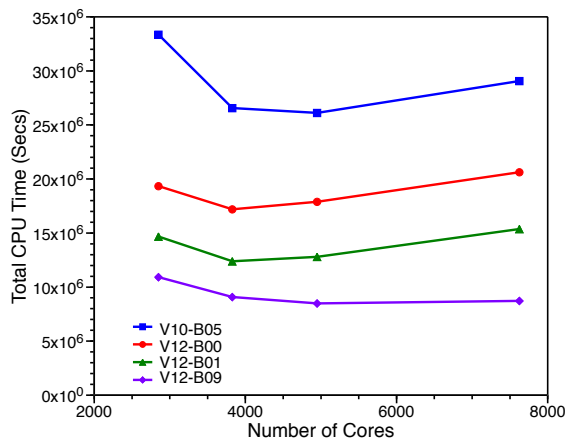


Figure 10. Total CPU time for the same test cases evaluated in Fig. 9 running on various numbers of Franklin cores.

Several of these methods can easily be explored with MFDn. For example, while MFDn has some components that are specific for the HO basis, it is straightforward to switch to another single-particle basis with the same symmetries but with different radial wavefunctions. Alternative truncation schemes such as Full Configuration Interaction (FCI) basis spaces are also implemented and easily switched on by appropriate input data values. These flexible features have proven convenient for addressing a wide range of physics problems.

There are additional suggestions from colleagues that are worth exploring as well such as the use of wavelets for basis states. These suggestions will clearly involve significant research efforts to implement and assess.

7. Performance of MFDn

We present measures of MFDn performance in Figs. 9 and 10. Fig. 9 displays the performance characteristics of MFDn from the beginning of the SciDAC-UNEDF program to the present, roughly a 2 year time span. Many of the increments along the path of improvements have been documented [11, 18, 19].

Fig. 9 displays the timings for major sections of the code as well as the total time for a test case in ^{13}C using a NNN potential on 4950 Franklin processors. The timings are specified for MFDn versions that have emerged during the SciDAC-UNEDF program. The initial version tested, V10-B05, represents a reasonable approximation to the version prior to SciDAC-UNEDF. We note that the overall speed has improved by about a factor of 3. Additional effort is needed to further reduce the time to evaluate the many-body Hamiltonian H and to perform the matvec operations as the other sections of the code have undergone dramatic time reductions.

We present in Fig. 10 one view of the strong scaling performance of MFDn on Franklin. Here the test case is held fixed at the case shown in Fig. 9 and the number of processors is varied from 2850 to 7626. Due to memory limitations associated with the very large input NNN data file (3 GB), scaling is better than ideal at (relatively) low processor numbers. At the low end, there is significant redundancy of calculations since the entire NNN file cannot fit in core and must be processed in sections. As one increases the number of processors, more memory becomes available for the NNN data and less redundancy is incurred. At the high end, the scaling begins to show signs of deteriorating due to increased communications time relative to computations.

The net result is the dip in the middle which we can think of as the "sweet spot" or the ideal number of processors for this application. Clearly, this implies significant preparation work for large production runs to insure maximal efficiency in the use of limited computational resources. For the largest feasible applications, this also implies there is high value to finding a solution for the redundant calculations brought about by the large input files. We are currently working on a hybrid OpenMP/MPI version of MFDn, which would significantly reduce this redundancy. However, at the next model space, the size of the input file increases to 33 GB, which we need to process in sections on Franklin.

8. Conclusions and Outlook

Microscopic nuclear structure/reaction physics is enjoying a resurgence due, in large part, to the development and application of *ab initio* quantum many-body methods with realistic strong interactions. True predictive power is emerging for solving long-standing fundamental problems and for influencing future experimental programs.

We have focused on the no core shell model (NCSM) and the no core full configuration (NCFC) approaches and outlined our recent progress. Large scale applications are currently underway using leadership-class facilities and we expect important progress on the path to detailed understanding of complex nuclear phenomena.

We have also outlined the challenges that stand in the way of further progress. More efficient use of memory, faster I/O and faster eigensolvers will greatly aid our progress.

Acknowledgments

This work was supported in part by DOE grants DE-FC02-09ER41582 and DE-FG02-87ER40371. Computational resources are provided by DOE through the National Energy Research Supercomputer Center (NERSC) and through an INCITE award (David Dean, PI) at Oak Ridge National Laboratory and Argonne National Laboratory.

References

- [1] P. Navrátil, J. P. Vary and B. R. Barrett, Phys. Rev. Lett. **84**, 5728 (2000); Phys. Rev. C **62**, 054311 (2000).
- [2] P. Maris, J. P. Vary and A. M. Shirokov, Phys. Rev. C. **79**, 014308(2009), arXiv 0808.3420.
- [3] P. Navrátil, J.P. Vary, W.E. Ormand, B.R. Barrett, Phys. Rev. Lett. **87**, 172502(2001)
- [4] E. Caurier, P. Navrátil, W.E. Ormand and J.P. Vary, Phys. Rev. C **66**, 024314(2002); A. C. Hayes, P. Navrátil and J. P. Vary, Phys. Rev. Lett. **91**, 012502 (2003).
- [5] A. Negret, et al, Phys. Rev. Lett. **97**, 062502 (2006).
- [6] S. Vaintraub, N. Barnea and D. Gazit, nucl-th 0903.1048
- [7] P. Navrátil, V. G. Gueorguiev, J. P. Vary, W. E. Ormand and A. Nogga, Phys. Rev. Lett. **99**, 042501(2007); nucl-th 0701038.
- [8] A. M. Shirokov, J. P. Vary, A. I. Mazur and T. A. Weber, Phys. Letts. B **644**, 33(2007); nucl-th/0512105.
- [9] J.P. Vary, The many-fermion dynamics shell-model code, 1992, unpublished.
- [10] J.P. Vary and D.C. Zheng, The many-fermion dynamics shell-model code, ibid. 1994, unpublished.
- [11] P. Sternberg, E.G. Ng, C. Yang, P. Maris, J.P. Vary, M. Sosonkina and H. V. Le, Accelerating Configuration Interaction Calculations for Nuclear Structure, Conference on High Performance Networking and Computing, IEEE Press, Piscataway, NJ, 1-12. DOI= <http://doi.acm.org/10.1145/1413370.1413386>
- [12] S. K. Bogner, R. J. Furnstahl, P. Maris, R. J. Perry, A. Schwenk and J. P. Vary, Nucl. Phys. A **801**, 21 (2008) [arXiv:0708.3754 [nucl-th]].
- [13] T. Dytrych, K.D. Sviratcheva, C. Bahri, J.P. Draayer and J.P. Vary, Phys. Rev. Lett. **98**, 162503 (2007); Phys. Rev. C **76**, 014315 (2007); J. Phys. G. **35**, 123101 (2008); and references therein.
- [14] A. Negoita, to be published.
- [15] R. Roth and P. Navrátil, Phys. Rev. Lett. **99**, 092501 (2007).
- [16] W.E. Ormand, Nucl. Phys. A **570**, 257(1994).
- [17] M. Honma, T. Mizusaki and T. Otsuka, Phys. Rev. Lett. **77**, 3315 (1996). [arXiv:nucl-th/9609043].
- [18] M. Sosonkina, A. Sharda, A. Negoita and J.P. Vary, Lecture Notes in Computer Science, **5101**, Bubak, M.; Albada, G.D.v.; Dongarra, J.; Sloot, P.M.A. (Eds.) pp. 833–842 (2008).
- [19] N. Laghave, M. Sosonkina, P. Maris and J.P. Vary, paper presented at ICCS 2009, to be published.